*Vision Res.* Vol. 31, No. 5, pp. 787–803, 1991
Printed in Great Britain. 

0042-6989/91 $3.00 + 0.00


# TEMPORAL PHASE RESPONSE OF THE SHORT-WAVE CONE SIGNAL FOR COLOR AND LUMINANCE

CHARLES F. STROMEYER III, RHEA T. ESKEW JR and RICHARD E. KRONAUER
Division of Applied Sciences, Harvard University, Cambridge, MA 02138, U.S.A.

LOTHAR SPILLMANN
Neurologische Universitätsklinik, Abteilung für Neurophysiologie, Hansastr. 9, D-7800 Freiburg i.Br., F.R.G.

(*Received* 21 *June* 1989; *in revised form* 30 *July* 1990)

**Abstract**—A chromatic discrimination paradigm was used to measure the temporal phase of the S (short-wave cone) signal relative to the L − M (long-wave cone minus middle-wave cone) signal. Suprathreshold equiluminant red-green flicker that stimulates the L − M mechanism was presented on a steady, intense yellow-green adapting field. Violet flicker that stimulates the S cones was added to the red-green flicker at different temporal phase angles, and the violet modulation depth was varied to achieve a chromatic discrimination threshold. A template was fitted to the data relating thresholds to phase: the location of the template symmetry axis showed that the S signal lagged L − M by about 75–90° at 10 Hz. This is about one half the phase lag obtained for luminance or motion discrimination. The phase discrepancy shows that there are separate luminance and chromatic mechanisms receiving S cone inputs. The hue of the flicker in the present study varied strongly with phase angle, with the positive and negative excursions of the S cone signal producing a reddish-blue and greenish-yellow, respectively, and these colors combined with the reddish and greenish hues produced by the L − M signal. The observed phase shift, and measured color appearance of the combined flicker, account for the colors seen on a radially segmented disk of Munsell hues when rotated: the colors differ strikingly depending on the direction of rotation.

S cones  Temporal phase  Chromatic discrimination  Color appearance  Opponent mechanisms

## INTRODUCTION

In the contemporary expression of opponent-color theory, the S or short-wave cones provide input to three mechanisms: a blue–yellow chromatic mechanism (Hurvich & Jameson, 1957; Thornton & Pugh, 1983a), a red–green chromatic mechanism (Hurvich & Jameson, 1957; Boynton, Nagy & Olson, 1983), and a luminance mechanism (Stockman, MacLeod & DePriest, 1987; Lee & Stromeyer, 1989). The present study documents the temporal phase lag of S cone signals relative to those of the middle-wave (M) and long-wave (L) cones, when the different mechanisms are stimulated, and thus provides evidence for separate pathways receiving S cone inputs.

### *Detection mechanisms and color appearance*

Detection experiments have demonstrated a mechanism that responds to the linear difference of L and M cone signals (Boynton & Kambe, 1980; Thornton & Pugh, 1983b; Stromeyer, Cole & Kronauer, 1985), and this mechanism is thought to produce hue sensations that are predominantly red and green (Boynton & Kambe, 1980; Krauskopf, Williams & Heeley, 1982; Thornton & Pugh, 1983b). However, under conditions where the S cones probably do not contribute (Middleton & Holmes, 1949), such as for 1′ or 2′ stimuli viewed with the center of the fovea, all colors seen can be matched with stimuli that fall along a line in chromaticity space that intersects the spectrum locus in the orange (595–625 nm) and blue–green (487–490 nm) regions. Drum (1989) argues that an incremental M-cone stimulus on a white field yields a "bluish cyan" signal. Thus, the L − M signal may give rise to sensations of orange and blue–green under some conditions rather than to unique red and green. Mollon (1982) provides a detailed discussion of this topic.

Modulating the S cones only (along a tritanopic confusion line) produces a sensation not

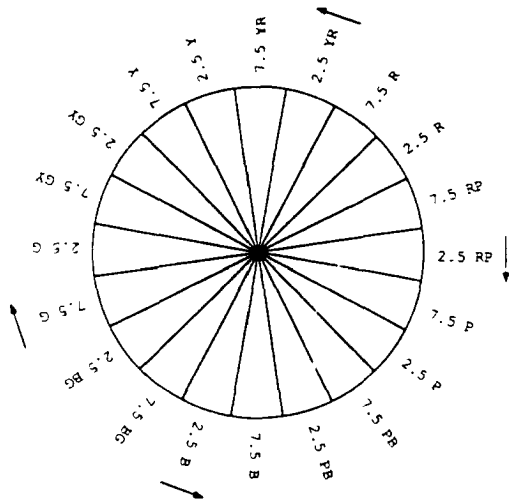


Fig. 1. Disk of Spillmann and Neumeyer (1984), originally made of Munsell papers of constant chroma and value (6). When spun at 7–9 Hz in white light, the flickering disk alternates in predominant color between green and purple for clockwise rotation and orange and turquoise for counterclockwise rotation. Designations which are marked with arrows represent the approximate hues seen when the disk is spun in the direction of the arrows. [Redrawn from Spillmann & Neumeyer (1984). Colored versions of the disk are available from L.S.]

of unique blue and yellow but of red–blue and green–yellow (Krauskopf et al., 1982; Boynton et al., 1983). The blue and yellow components may be caused by an S cone input to the blue–yellow mechanism, in which S signals oppose a sum of L and M signals (Hurvich & Jameson, 1957), while the red and green components may be caused by an S input to the red–green mechanism, in which S signals support L signals and oppose M signals (Hurvich & Jameson, 1957 Boynton et al., 1983).

In the present study, we combined sinusoidal L − M flicker and S flicker in various temporal phase relationships, and used the appearance of the combined stimulus to measure the relative S cone phase lag in the red–green mechanism. In addition, we measured the relative S cone phase lag for a luminance discrimination task with S and L + M flicker (with L and M modulated in phase), and compared the luminance and chromatic phase lags as a function of S cone light-adaptation level. Finally, using the same L + M stimuli, we made limited phase measurements for yellow–blue chromatic discrimination. The procedure separated the S cone input to the luminance, red–green and blue–yellow pathways. The results also provide an explanation for an interesting color appearance phenomenon, described next.

*The color-circle sequence effect*

One goal of this study was to explain a phenomenon originally observed by a Miss Olive E. Peake (Hartridge, 1949, p. 148), which was independently rediscovered in 1974 by one of us (L.S.), using the colored disk illustrated in Fig. 1. The disk consists of 20 sectors of Munsell papers of constant chroma and value, arranged in the sequence of the color circle (Spillmann, 1974). When illuminated with white light, and spun at 7–9 Hz, the flickering disk alternates in predominant color between green and purple for clockwise motion, while for counterclockwise motion it alternates between orange and turquoise (Spillmann & Neumeyer, 1984; Spillmann, 1990). The colors depend not on motion, but rather on the temporal sequence of chromatic stimulation, for the colors are equally impressive when a small region is viewed through a reduction tube (Spillmann & Neumeyer, 1984). When the whole disk is viewed, the colors appear mottled because opposite sectors are in counterphase chromatic modulation. In the present experiment, the colors are produced with a spatially uniform flickering field which contains no motion.

Spillmann and Neumeyer (1984) suggested that the colors could be explained by temporal masking between different classes of chromatic LGN cells. The present experiments support a simpler view of this phenomenon.

We postulate that the equiluminant disk produces two basic signals. One signal originates in the S cones, while the second signal, L − M, represents the difference of L and M cone signals. There may be a phase shift between the S and L − M signals. The speed of the disk that yields the maximal color difference for the two directions of rotation will be such that the S and L − M signals are approximately in-phase for one direction of rotation and approximately in antiphase for the opposite direction, thus producing optimal opponent hue cancellation and reinforcement. For example, if the red–blue color from the S signal is aligned in time with the green (or blue–green) color from the L − M signal, the signals producing the green and red hues will partially cancel leaving mostly blue; the signals for green–yellow and red (or orange) will then also be aligned in time and thus yield mostly yellow—therefore one direction of rotation will produce largely blue and yellow. The same argument shows that the other direc-

tion of rotation will produce largely red and green.

The disk has a complicated spatio-temporal waveform (see Discussion). The uniform sinusoidal flicker which we use for the phase measurements provides a simpler means of stimulating L − M and the S cones. After measuring phase lags with this stimulus, we determined the colors produced by each of these flicker signals singly and in combination with the other.

## METHODS

### *Stimulus and apparatus*

The stimulus was produced with an optical system (Lee & Stromeyer, 1989) incorporating three Tektronix 608 monitors with red, green and violet phosphors that were flickered sinusoidally. The stimulus was a uniform 2° disk, made up of light from the three monitors (red, green and violet at 320, 760 and 22 td respectively), superposed on the center of a 4.2° yellow-green adapting field (559 nm and 3000 td) seen in Maxwellian view. The adapting field was larger than the disk so as to adapt the fovea homogeneously. When not being flickered, the stimulus appeared as a 2° whitish disk with a yellow-green surround, even though the uniform yellow-green field underlay the disk. The red, green and violet monitors were filtered with, respectively, a Wratten 22 filter, a Wratten 55 filter and a 460-nm short-pass interference filter, and were optically combined by means of dichroic mirrors to reduce light loss. Spectral calibrations from 350 to 750 nm were made at the eyepiece with a monochromator (2 nm HBW) and radiometer. The violet monitor had a HBW of 423–459 nm and spectral centroid of 441 nm, based on quantal flux; for the green monitor, the HBW was 43 nm and the spectral centroid, 533 nm; and the red monitor had a spectrum of narrow bands with most energy at 627 nm and much less at 596, 618 and 707 nm. The violet light produced a quantal catch rate in the S cones equivalent to that produced by a monochromatic beam of 8.78 log quanta $\cdot$ deg$^{-2}\cdot$sec$^{-1}$ at 441 nm.

The L − M signal was produced by flickering the red and green lights in antiphase at equal luminance. To establish equiluminance, the red light was flickered at a fixed modulation, and the green modulation was adjusted to produce minimal apparent flicker. The other light components were present and steady. The settings were similar for all observers and did not change with temporal frequency (5–12.5 Hz), and so we set the red/green ratio to a constant value.

The stimuli are depicted in Fig. 2 within the equiluminant chromaticity diagram of MacLeod and Boynton (1979). Each axis is normalized by a steady luminance, L + M: the vertical axis represents S trolands (Boynton & Kambe, 1980) divided by luminance, i.e. S/(L + M), and the horizontal axis represents the trade-off of L and M at equal luminance—hence L/(L + M) = 1 − M/(L + M). In the Smith and Pokorny (1975) system, the heights of the L and M functions are set so that L + M = $V_\lambda$, but the scaling of S is arbitrary. The scaling of S cone excitation in S trolands used here differs from that of MacLeod and Boynton (the final coefficient in their transformation equation is here set to 1.0 instead of 0.01608); dividing by L + M prevents luminance changes from causing changes in chromaticity coordinates. The two arrows in Fig. 2 represent the "red-green" and the "violet" flickering lights, and their intersection represents the mean chromaticity of the field within the disk test area.

We ideally want the red-green flickering lights to stimulate only L − M and the violet flickering lights to stimulate only S cones. The degree to which this is achieved can be seen by calculating the cone contrasts of the two flickers (Stromeyer et al., 1985).

The fixed-amplitude red-green flicker (Fig. 2) stimulates the M and L cones in antiphase at equiluminance, with L and M cone contrast of

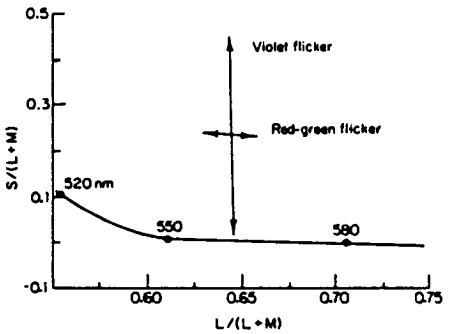


Fig. 2. The two stimulus components (with the violet at maximum) are plotted in the equiluminant chromaticity diagram of MacLeod and Boynton, which depicts L − M stimulation on the horizontal axis and S stimulation on the vertical axis. A portion of the spectrum locus is also plotted. The assumed cone fundamentals are those of Smith and Pokorny.

3%, as $|\Delta L/L| = |-\Delta M/M| = 0.03$.* This level is estimated to be 10–20 × threshold at 1–3 Hz (Stromeyer et al., 1987). The red–green flicker also stimulates the S cones at about 1% contrast; this level is likely to be subthreshold for the S cones, owing to their low contrast sensitivity (Stiles, 1953).

The violet flicker at maximum value stimulates S cones at 94% contrast. It also weakly stimulates M more than L (Fig. 2), resulting in 0.2% chromatic contrast, i.e. the projection of the violet light vector onto $\Delta L/L - \Delta M/M$ is equivalent to $|\Delta L/L| = |-\Delta M/M| = 0.002$. In addition the maximal violet flicker produces luminance flicker of 0.6%, which cannot be shown in this equiluminant diagram. For the phase measurements, the violet flicker was generally well below its maximum.

On each presentation, red–green and violet flicker of the same frequency were ramped on and off together for 339 ms with a raised cosine envelope, and were held constant for 678 ms in between (the presentation was expanded 2 × for 1 Hz flicker). Stimuli were controlled with an Innisfree Image Synthesizer, function generators and a PDP 11/34a computer with 12-bit DACs. The monitor frame rate was 106.2 Hz, and all phosphors decayed to 1/10 in < 1.2 msec. Stimuli were viewed monocularly through a 3 mm artificial pupil, achromatizing lens (that corrected chromatic aberration), and relay lenses, with the head stabilized with a bite bar. The observer fixated the center of the whitish disk.

*Observers*

Observers were three of the authors, who scored well on the Farnsworth–Munsell 100-Hue Test.

*Procedure: phase measurements*

The relative phase of the S and L − M signals was measured with a 2AFC staircase. On each trial, the fixed, equiluminant red–green flicker was presented in both temporal intervals, and the violet flicker was added in one interval at temporal phase angle $\phi$ (referenced relative to the red peak of the red-green flicker) and was added in the other interval at the opposite angle, $\phi$-180°. The amplitude of the violet flicker was the *same* in both intervals, but varied between trials. The value of $\phi$ was fixed for each run. The observer discriminated between two intervals, where the only stimulus difference was the relative phase of the violet and red–green flicker: $\phi$ vs $\phi - 180°$. The interval containing $\phi$-phase flicker was arbitrarily defined as the correct interval; auditory feedback was given after each trial. Because the colors associated with $\phi$ and $\phi - 180°$ vary with $\phi$, the observer was required to learn in the first several trials what hue to associate with $\phi$ (see Results). The amplitude of the violet flicker was lowered 0.10 log unit after two correct responses and raised the same amount after each incorrect response, a procedure that estimates 71% correct response (Wetherill, 1963). Two staircases were randomly interleaved in each run: the first two reversals of each staircase were discarded, and the subsequent 4–6 reversals were saved. Each threshold estimate was the geometric mean of 2–10 staircases.

Similar templates were also measured using a "luminance" criterion, to compare the relative phase of S and a luminance, L + M, signal. For these measurements, the red and green flickering beams were first placed in-phase, and the observer adjusted the amplitude ratio so as to see no red-green chromatic modulation. (It was necessary to adjust the amplitude ratio, since simply placing the beams in-phase would not in general eliminate the red-green modulation.) For this initial setting the flicker was 3 Hz and highly suprathreshold. For the actual phase measurements L and M were modulated at 1.7% contrast and 10 Hz. [There should be little phase shift between the L and M signals in going from 3 to 10 Hz on the 559-nm adapting field (Stromeyer, Cole & Kronauer, 1987).]

*Procedure: color matching*

The initial measurements with the violet and red-green flicker show which angle $\phi$ and its phase-opposite, $\phi - 180°$, produce the most discriminable colors. Next, at each temporal frequency, the phase was set at these two optimal angles, the violet flicker was fixed at maximum and the observer matched the colors seen. The

*Chromaticity diagrams like that of MacLeod and Boynton (1979), make no provision for adaptation, since luminance (the denominator term for the two axes) is defined as a sum of L and M with fixed weights. However, the effectiveness of L and M varies with adaptation of the L and M cones (Eisner & MacLeod, 1981; Stromeyer et al., 1985, 1987): the luminance mechanism responds to a weighted sum of $\Delta L/L$ and $\Delta M/M$ (Stromeyer et al., 1987). For the flicker vectors in Fig. 2, the sum L + M actually varies slightly, while $\Delta L/L + \Delta M/M$ is constant; the plotted vectors thus are projections into the constant L + M plane and hence are slightly foreshortened. For the calculations in Fig. 9, we assumed that L + M was constant.

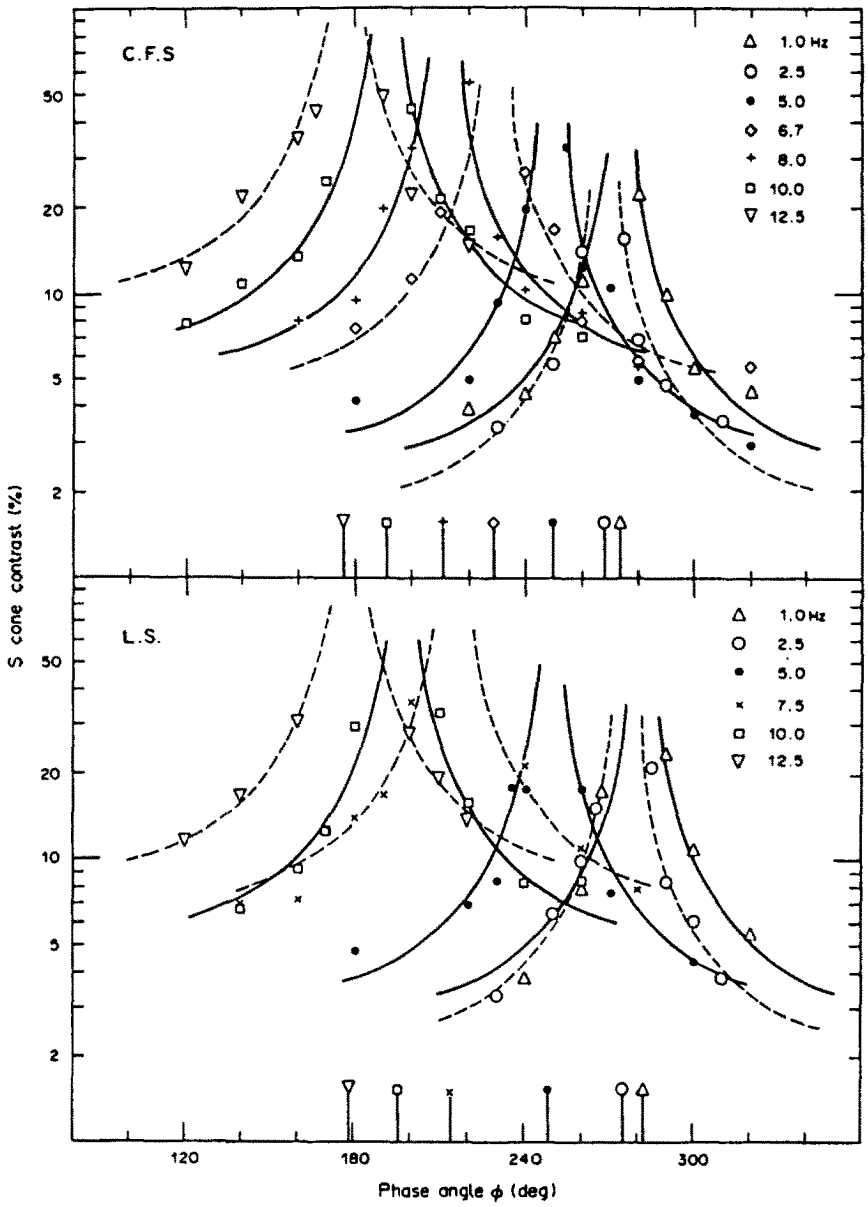


Fig. 3. Phase of the S cone signal measured relative to the L − M signal for chromatic vision, at various temporal frequencies. Data for each frequency show the S cone contrast of the violet flicker as a function of the phase angle $\phi$ (i.e. the threshold for discriminating $\phi$ from $\phi - 180°$ is plotted at each $\phi$). A template is fitted at each frequency—the symbols near the abscissa mark the symmetry axis of each template. A peak position of 270° (equivalent to 90°) indicates no phase shift between the S and L − M signals, whereas a position of $<270°$ indicates an advance of the violet stimulus, corresponding to a phase lag of the S cone signal.

*Munsell Book of Color* and the flickering fields were alternately viewed with the right and left eyes respectively. (The book was viewed with a mirror, so that the observer did not disturb his position on the bite bar.) The book was illuminated by a 200 W incandescent lamp and viewed through Wratten 78B and 80B filters, which closely approximates Illuminant C (Pokorny, Smith & Lund, 1978). Each Munsell patch subtended 1.0 by 1.2°, and the illuminance of the white background was 800 lx as viewed through the filters. After an initial perusal of the book for each match, selected chips were removed from the book and examined 5–12 at a time on the white background. The observer chose 1–3 chips that formed the best match, and the mean was determined.

## RESULTS

### *Phase measurements with L − M flicker*

We first measured the relative phase of the S and L − M signals. Figure 3 shows the threshold contrast of the violet flicker, ΔS/S, required for chromatic discrimination when the violet flicker is added to the fixed, equiluminant red–green flicker at different phase angles, $\phi$, measured over the range of 1–12.5 Hz. Consider the red–green flicker to be in temporal cosine phase, with the peak of the red component represented at 0° on the abscissa (360° in Fig. 3). The abscissa then specifies the relative phase angle of the violet flicker $\phi$, with increasing values of $\phi$ representing points later in time relative to the peak of the red component (time increases rightward on the abscissa). Increasing the phase delay of the violet stimulus corresponds to a decrease in the relative lag of the S cone signal (see below). The contrast of the violet flicker was the same in both intervals of a trial, and was varied between trials. The threshold thus represents the violet contrast required for discriminating $\phi$ from $\phi - 180°$, plotted at phase $\phi$ in Fig. 3.

Discrimination will be best when the color signals due to S and L − M are, respectively, in-phase and in antiphase for the two temporal intervals, and discrimination will be worst when the signals are in quadrature phase (90° or 270°). (Placing the two signals in quadrature phase would leave no difference between the two temporal intervals, except in the order in which the peaks of the two signals occur, which presumably would contribute little to the discrimination.) Thus, if there were *no* phase shift between the S and L − M signals, discrimination would be best for $\phi = 0°$ and 180° and worst for $\phi = 90°$ and 270°, with sensitivity varying approximately as the absolute value of $\cos\phi$.

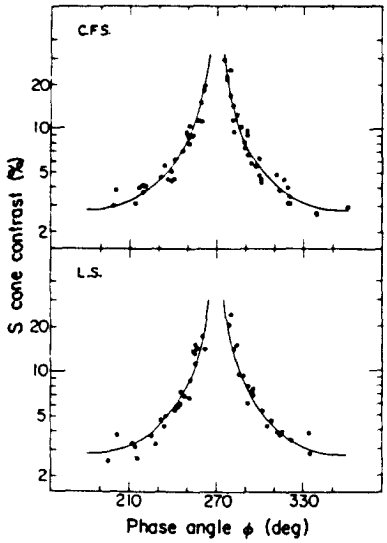


Fig. 4. The excellent fit provided by the phase template is shown here, where the data for all the conditions in Fig. 3 are replotted with the fitted templates moved into spatial coincidence.

In Fig. 3 we plot threshold, which is the inverse of sensitivity, and thus the thresholds vary approximately as $|\cos\phi|^{-1}$ (Lee & Stromeyer, 1989); the templates are of this form.* The excellent fit is shown in Fig 4, where the data for all the conditions in Fig. 3 are plotted with the fitted templates moved into spatial coincidence. Lindsey, Pokorny and Smith (1986) employed a similar template to accurately assess phase shifts.

For the data points on the left-hand side of each template in Fig. 3, the test interval containing violet flicker of angle $\phi$ appeared relatively more bluish and yellowish compared to the test interval containing violet flicker with the opposite angle, $\phi - 180°$, which appeared relatively more reddish and greenish. On the right-hand side of each template, this pairing of phase and color was reversed, for the $\phi$ stimulus on the left side is physically identical to the $\phi - 180°$ stimulus at the symmetrical template position on the right side, and conversely.

*The template is an approximation. The observer presumably responds to the effective difference of the vector sums of the flicker (violet and red–green) in the two intervals. Let the ΔS/S flicker amplitude be represented as S, relative to the fixed ΔL/L − ΔM/M amplitude. When these two stimulus vectors are combined at angles $\phi$ and $\phi - 180°$ in the two intervals, and the physiological phase shift is $\theta$, the resultant vector lengths for the two intervals are:

$$a = \{[1 - S\cos(\phi + \theta)]^2 + S^2\sin^2(\phi + \theta)\}^{1/2}$$

$$b = \{[1 + S\cos(\phi + \theta)]^2 + S^2\sin^2(\phi + \theta)\}^{1/2}.$$

We assume that $|a - b|$ is a constant at threshold. There is no closed-form solution for S, although exact numerical solutions can be obtained; note, however, that if we assume that $S = S_0\cos^{-1}\phi$ as specified by the template, then $a - b = 2S_0$, where $S_0$ is the threshold of the S cone mechanism. The divergence of the template from the true function is relatively small when S is small; that is, when the violet flicker at the template trough (point of maximal sensitivity) is effectively small relative to the red–green flicker. The divergence becomes appreciable only near the peak of the template (where the violet flicker is stronger), but this does not affect the estimated symmetry of the template.

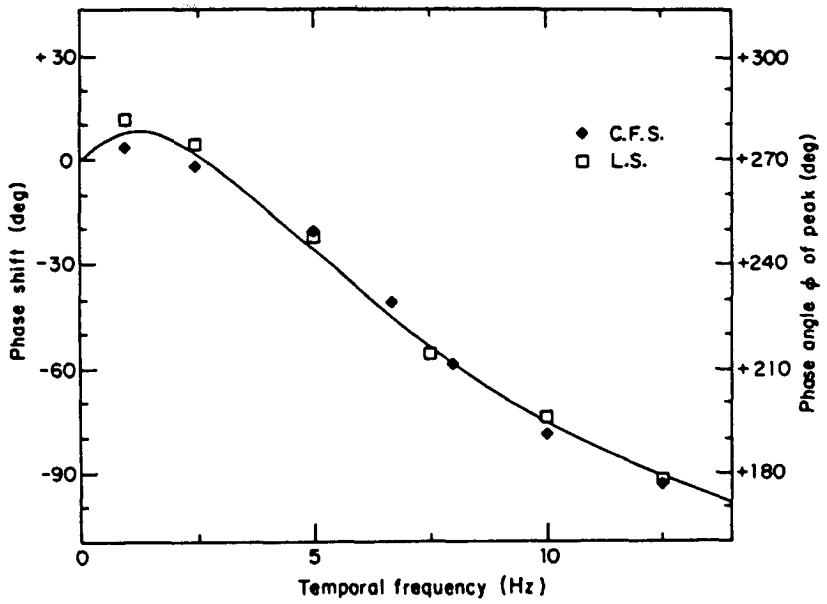


Fig. 5. Summary of phase measurements for the chromatic discrimination. The right ordinate depicts the horizontal position of the peak of the templates (Fig. 3) as a function of temporal frequency, while the left ordinate depicts the phase lag of the S cone signal relative to the L − M signal. The smooth curve is the phase transfer function described in the text. The S cone adapting level was 8.80 log quanta·deg$^{-2}$·sec$^{-1}$.

If there were no phase shift between the S and L − M signals, the template symmetry axis would be positioned at $\phi = 270°$. This condition approximately obtains at 1 Hz where we expect the angular phase to be small: the template axis for observers C.F.S. and L.S. is at 274° and 284°, respectively, indicating a small advance of the S signal relative to L − M, since the violet flicker (at the template peak) was presented 4° and 14° later in time relative to the 270° quadrature point. The fitted template reaches a minimum (maximal sensitivity) at $\phi \cong 0°$ and 180°. Thus at $\phi = 0°$, the S and L − M cone signals are approximately in-phase and the combined flicker appeared relatively more reddish and greenish (as shown by color matches reported below), while at $\phi = 180°$, the S and L − M cone signals are approximately in antiphase and the combined flicker appeared relatively more bluish and yellowish.

The template axis shifts progressively with increasing temporal frequency (Fig. 3), indicating an increasing relative phase lag of the S cone signal. This phase shift is plotted in Fig. 5. A simple delay of the S cone signal would be represented by a straight line passing through zero phase shift at zero Hz. The data deviate significantly from this characterization, most notably in the phase advances seen at 1 and 2.5 Hz but also in a clear deceleration for frequencies above 5 Hz. The solid curve represents a fit to these phase shift data in the form of a transfer function involving only real zeros and negative real poles. The function has a zero at 1.75 Hz and a triple pole at 7.9 Hz and is given mathematically by $(1.75 + if)/(7.9 + if)^3$, where $f$ is the test frequency in Hz and $i = \sqrt{-1}$. Since the number of poles exceeds the number of zeros by two, for large $f$ the phase lag is asymptotically 180°, unlike the ever-increasing phase lag of a simple delay function.

Although the violet flicker does not solely stimulate the S cones, the following considerations indicate that the stimuli do produce the desired phase-shifted signals between S cones and L − M. First, at the minima of the curves in Fig. 3 the violet flicker produces 2–10% S cone contrast. This violet flicker produces corresponding M and L cone contrasts of only 0.016–0.082% and 0.009–0.043%, respectively, which are likely to be too small to contribute to the discrimination. Second, these contrast values show that the violet flicker does stimulate the M cones slightly more than the L cones, thus producing a weak L − M signal. However, if this signal mediated discrimination, then the minima of the phase curves would be at $\phi = 0°$ and 180° for all frequencies. The results for 10 Hz (Fig. 3) clearly contradict this, since the threshold is highest near 180°, rather than being minimal. Third, the template axis shifts

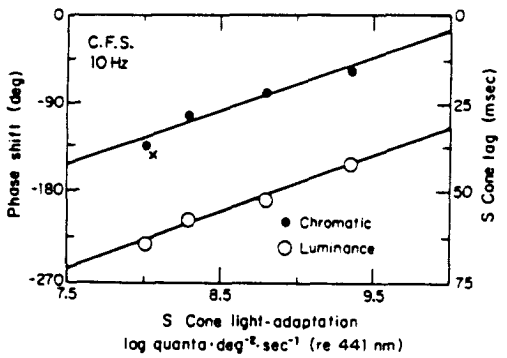


Fig. 6. Relative phase shift (left ordinate) and S cone lag (right ordinate) as a function of S cone adapting level. The filled symbols are for the same chromatic discrimination as in Fig. 3 (S and L − M flicker). The open symbols are for a luminance discrimination (S and L + M flicker). All stimuli were at 10 Hz. (The cross is from a control experiment.) S signals are about 100° more delayed for the luminance judgment. However, the chromatic and luminance judgments are equivalently affected by changing the S cone adapting level (the slopes are equal).

progressively with temporal frequency over the whole measured range.

*Phase shift and S cone light adaptation: chromatic and luminance discrimination*

Before describing the color matches for the L − M and S stimuli, we shall briefly consider how the lag of the S cone signal depends on the light adaptation of the S cones, since the measurements thus far have been obtained only at one level. Stockman et al. (1987) and Lee and Stromeyer (1989) showed that light adaptation strongly affected the lag of the S signal for luminance judgments. To see if the lag for the chromatic task is similarly affected, we measured templates at 10 Hz, using the same chromatic discrimination paradigm, and we reconfirmed the luminance phases with a luminance discrimination paradigm. S cone adapting level was independently varied (with M and L held almost constant) by placing ND filters before the violet monitor or by adding uniform 442 nm light to the field.

Luminance templates were measured with in-phase L + M, yellow, flicker (Methods) combined with the violet flicker, as before. The observer discriminated which interval had the more vigorous brightness flicker, or apparent "agitation", while ignoring any color difference (an easy task with the two-interval comparison).

Each point in Fig. 6 is based on a complete template (the cross is from a control experiment*). The results show that, at 10 Hz, the S cone lag is larger for the luminance than for the chromatic judgments: the vertical difference between the two lines is about 100°, corresponding to 28 msec at 10 Hz. However, the change in lag with adaptation level is similar for the two judgments, and thus light adaptation affects the S cone signals at an early stage (perhaps at the level of the cones themselves), before the signals split into luminance and chromatic pathways. For both judgments, the S cone lag decreases about 17 msec as the adapting level is raised 1.0 log unit over this range of intensities. Lee and Stromeyer (1989) obtained a value of 17 ms for observer C.F.S. using a motion discrimination paradigm, while Stockman et al. (1987) obtained a value of ~17 msec for photometric nulls (mean of 3 observers).

*Phase measurements with luminance and yellow–blue flicker*

The red + green flickering lights used for the luminance judgments were adjusted to produce no red–green flicker; however, they might have produced some yellowish flicker within the central, whitish test region. The observer might have inadvertently based his judgment on this color difference rather than on luminance. However, the following results suggest that this is unlikely. The template was remeasured with the same "luminance" stimuli with minor changes: the green light* was narrow-band 540 nm; the mean radiances of the green and red lights were 330 and 210 td, with M and L modulated in phase at 1.4%; and the S cone adapting level was 8.80 log quanta·deg$^{-2}$·sec$^{-1}$. Figure 7 shows two templates measured with identical stimuli at 3 Hz: for the left, "luminance" template, the observer discriminated, as before, which interval had the more vigorous luminance flicker; for the right template, he discriminated which interval had the greater yellow–blue flicker. (The color judgments were easy at 3 Hz, while at >5 Hz the colors were too weak for

*As S cone adapting level is reduced in steps (Fig. 6), the green component of the red–green chromatic flicker increasingly stimulates S cones: $\Delta S/S \cong 0.3$, 1.0, 3.1, 5.9% for the chromatic task. (Values were 3× less for the luminance task.) Even at the lowest adapting level where the artifact is largest, the template did not appear distorted, and sensitivity was near maximal at $\phi = 90°$ and 270° where the artifact can have no effect. The chromatic template, nevertheless, was remeasured near the lowest adapting level (cross, Fig. 6) with a 540 nm interference filter (10 nm HBW) placed before the green monitor, reducing $\Delta S/S$ of the green light to 1.5% − 20× below the level of the violet flicker at the template troughs.

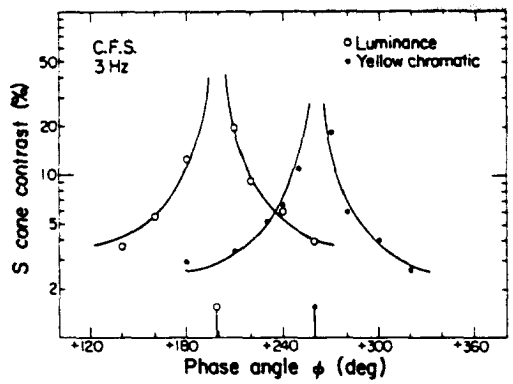


Fig. 7. Templates measured at 3 Hz using identical stimuli and a luminance or yellow chromatic criterion. Stimuli were similar to those used for the previous luminance judgments: S and L + M flicker. For the yellow chromatic judgments, the observer discriminated the yellow–blue content of the combined flicker, while ignoring brightness flicker; for the luminance judgments, he attended only to the brightness flicker. The templates are clearly separate, because sensitivity for each type of judgment is maximal where the other is approximately least sensitive.

reliable judgments.) On the left-hand side of each template, the interval corresponding to $\phi$ had the greater apparent modulation. Thus the yellow–blue flicker was stronger when the violet light and long-wave "yellow" light were in *antiphase* ($\phi = 180°$). The luminance flicker was also stronger when the lights were in antiphase (since $\phi = 180°$ is on the left-hand side of the luminance template), confirming the conclusion of Stockman et al. (1987) and Lee and Stromeyer (1989) that the S cones contribute to luminance with negative sign. Thus, the S signal is negative with respect to M and L for both the luminance and yellow–blue mechanisms. The novel feature is that the peaks of the two templates are widely separated (peaks at 199 and 260°). Thus the luminance and yellow–blue mechanism are each maximally sensitive where the other has low sensitivity, and the two mechanisms are clearly separable. Measurements (not shown) for a second observer, R.T.E., were similar, with peaks at 198 and 268°. (The M and L cones were modulated at a slightly higher level, 1.8%, for R.T.E.)

### *Color matching*

In the yellow–blue task the red and green lights were in-phase, and the stimulus variation was largely restricted to yellow and blue. When the red and green lights were in antiphase (Fig. 3) the colors seen were more varied, and this section describes these colors.

The left and right minima of each template in Fig. 3 indicate the two phase angles at which the violet flicker produces the most discriminable colors when combined with the equiluminant red–green flicker. For the present color matches, the violet flicker was fixed at its maximum value (94% S cone contrast), and presented with the red–green flicker at these two phase angles, at different temporal frequencies. Using Munsell chips, the observer matched the colors seen in the central 2° flickering disk. Matches were also made when the violet or red–green light was flickered alone with the other component maintained at zero modulation; here the colors were weaker, especially for the red–green flicker, and matches could be made at only low temporal frequencies. (The colors ought to be stronger for the in-phase S and L − M flicker, since the red and green hues from each flicker component would partially add.) Observers found it relatively easy to judge the predominant alternating colors of the flicker, as if the appearance varied as a square-wave rather than a sine-wave.

The matches (Tables 1 and 2) show several trends. First, increasing temporal frequency reduces the saturation or chroma (indicated by the last number specifying each match); this tendency is more pronounced for observer C.F.S. than for L.S. Second, the saturation of the colors is stronger for the violet and red–green flickering lights in combination than for either alone (Table 1 vs Table 2). Third, the hue varies little with temporal frequency, and thus we have calculated the mean hues, combining temporal frequencies. The violet light flickering alone appears purple (red–blue) and yellow or green–yellow (Table 2). The red–green lights flickering alone appear reddish-orange and green or slightly bluish-green, indicating that the L − M signal did not produce unique red and green (see Introduction). When the violet and red–green lights are flickered together with $\phi$ set so that the S and L − M signals are in-phase (bottom panel Table 1), then the red–blue (+S) and reddish-orange (M − L) produced by the two flickering sources combine as a red–purple, and the yellow or greenish-yellow (−S) and green (L − M) produced by the two sources combine as a green–yellow. When the violet and red–green lights are combined in the opposite phase so that the S and L − M signals are in antiphase (top panel Table 1), then the yellow or greenish-yellow (−S) and reddish-orange (L − M) produced by the two sources combine as a yellow, and the red–blue (+S) and

Table 1. Munsell matches (specifying in order: hue, value and chroma) of colors produced by violet and red-green flickering lights, combined in phase angle $\phi$ so that S and L − M chromatic signals are in antiphase (top panel) and in phase (bottom panel)

| | Yellows | | Blues | |
|---|---|---|---|---|
| Hz | C.F.S. | L.S. | C.F.S. | L.S. |
| 1.0 | 7.5Y 8.5/12 | 5Y 8.5/13 | 5BP 8/6 | 5PB 6.5/9 |
| 2.5 | 6.3Y 8.5/13 | 3.8Y 8.5/13 | 6.3B 8/5 | 3.8PB 7/8 |
| 5.0 | 6.3Y 8.5/10 | 2.5Y 8.3/12 | 2.5PB 8/4 | 3.8PB 7/8 |
| 7.5 | 6.3Y 9/6 | 5Y 8.5/9 | 6.3B 9/2 | 5PB 6.5/7 |
| 10.0 | 7.5Y 9/5 | 2.5Y 8.5/9 | 5PB 9/2 | 3.8PB 6/8 |
| Mean hue | 6.8Y | 3.8Y | 1.0PB | 4.3PB |
| | Green–yellows | | Red–purples | |
| Hz | C.F.S. | L.S. | C.F.S. | L.S. |
| 1.0 | 5GY 8/10 | 3.8GY 7.5/12 | 10P 8/6 | 5RP 7/9 |
| 2.5 | 8.8GY 8/9 | 3.8GY 7/12 | 1.2RP 7.5/6 | 3.8RP 7/10 |
| 5.0 | 5 GY 8/9 | 5GY 7/12 | 8.8RP 8/4 | 3.8RP 7/10 |
| 7.5 | 2.5GY 9/5 | 2.5GY 6.6/8.6 | 5RP 8/4 | 6.3RP 8/6 |
| 10.0 | 2.5GY 9/6 | 6.3GY 7/10 | 10P 8/4 | 3.8RP 8/6 |
| Mean hue | 4.8GY | 4.3GY | 3.0RP | 4.5RP |

green (M − L) produced by the two sources combine as a slightly purplish-blue.

## DISCUSSION

### *Colors seen on the spinning disks and in this experiment*

One of our goals was to mimic the spinning chromatic disk of Spillmann (1974) using a simpler stimulus that sinusoidally modulates the S cones and L − M. Table 3 summarizes the hues seen using spinning disks in several studies and the uniform flicker in the present study. The disks were made of Munsell matte papers of chroma and value of 6 and were spun at 7–9 Hz. The hues seen on the spinning disks were matched with the 85 chips of the Farnsworth–Munsell 100-Hue test or Munsell chips of constant chroma and value (6). The disks varied between the studies: Spillmann and Neumeyer (1984) used 20 sectors covering the hue circle (Fig. 1); the disk of Davidoff, Aspinall and Hill (1978) had 10 sectors; Spillmann (1990) used 4 sectors, 5RP, 5YR, 5G, 5B, which were meant to reflect the colors typically seen with the 20-sector disk; and Hill, Rodger and Smalridge (1980) used 3 sectors, 5RP, 5G, 5B. Table 3 shows the average Munsell matches for the two directions of rotation. The bottom two rows show the means of our hue matches (Table 1) for combined violet and red-green sinusoidal flicker. In general, the colors seen are qualitatively similar for the disks and for our uniform flicker, being strongly bluish and yellowish vs

Table 2. Munsell matches of colors produced by the violet flickering light (top panel) and the red-green flickering light (bottom panel)

| | Violet flickering light | | | |
|---|---|---|---|---|
| | Yellows | | Purples | |
| Hz | C.F.S. | L.S. | C.F.S. | L.S. |
| 1.0 | 2.5GY 8/12 | 5.8Y 8.5/13 | 2.5P 8/4 | 7.5P 8/7 |
| 2.5 | 2.5GY 8/12 | 3.8Y 8.5/11 | 2.5P 8/4 | 7.5P 8/5 |
| 5.0 | 2.5GY 8/10 | — | 2.5P 8.5/3 | 8.8P 8/6 |
| 7.5 | 2.5GY 9/4 | — | 2.5P 8.5/3 | 5.8P 8/4 |
| Mean hue | 2.5GY | 4.8Y | 2.5P | 7.4P |
| | Red-green flickering light | | | |
| | Oranges | | Greens | |
| Hz | C.F.S. | L.S. | C.F.S. | L.S. |
| 1.0 | 1.2YR 8/4 | 3.8YR 8/7 | 1.2BG 9/3.5 | 5.0G 8/5.3 |
| 2.5 | 1.2YR 8/4 | 3.8YR 8/7 | 1.2BG 9/3.5 | 6.8G 8/6 |
| 5.0 | 1.2YR 8.5/3 | 6.2YR 8/8 | 6.8G 9/1 | — |
| Mean hue | 1.2YR | 3.4YR | 9.7G | 5.9G |

Table 3. Average Munsell hue seen on sectored disks for the two directions of rotation (left and right panels) and on our flickering display (from Table 1)

| | | | | |
|---|---|---|---|---|
| Spillmann: | 20 sector | 2.5YR | 2.5B | 2.5RP 7.5G |
| | 4 sector | 2.5YR | 2.5B | 7.5RP 10.0G |
| Davidoff et al. | | 3.0YR | 7.5B | 9.5RP 9.0GY |
| Hill et al. | | 2.4YR | 8.3BG | 3.9RP 6.6GY |
| Present: | L.S. | 3.8Y | 4.3PB | 4.5RP 4.3GY |
| | C.F.S. | 6.8Y | 1.0PB | 3.0RP 4.8GY |

purplish and greenish, despite differences in adaptation conditions. The only substantial difference is the absence of redness in the present "yellow" hues.

We used our stimulus because it was simpler, provided better isolation of the S and L − M signals, and allowed us to vary independently the relative phase of the two signals at each temporal frequency. We shall now consider a more complex stimulus, the 4-sector disk of Spillmann (Table 3), to assess whether a phase shift between the S and the L − M signals can explain the colors seen there. In what follows we shall describe the "effective chromaticity", which is the vector sum of the phase-shifted cone signals, calculated for the temporal sequence of stimulation at a fixed arbitrary reference point on the retina.

The left two panels in Fig. 8 show the cone stimulation produced by the temporal sequence of the four 90° Munsell sectors, 5RP, 5YR, 5G, 5B, over two cycles of revolution. These values were calculated on the basis of the Smith and Pokorny fundamentals, using the CIE Munsell data for the standard Illuminant C employed by Spillmann (Newhall, Nickerson & Judd, 1943, tabulated in Wyszecki & Stiles, 1982). The sine-wave in the top panel shows the Fourier fundamental of the L − M stimulus, ΔL/L − ΔM/M, while the sine-wave in the bottom panel shows the fundamental of the S stimulus, ΔS/S. Reversing the spin of the disk (moving from right to left within a panel in Fig. 8), reverses the temporal phase relationship between the L − M and S stimuli. The stimulus fundamentals are $\phi = 129°$ different in phase. If the disk is spun sufficiently fast, the S signal will lag behind the L − M signal, bringing the S and L signals more closely into phase for one direction of rotation of the disk and more closely into

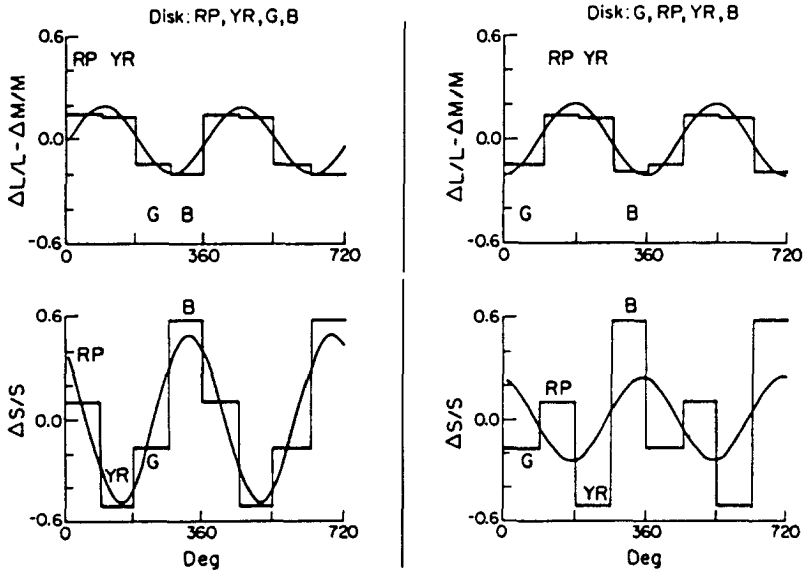


Fig. 8. The cone stimulation produced by the two 4-sector disks used by Spillmann (1988). Left panels: disk with Munsell sectors in sequence of color circle, 5RP, 5YR, 5G, 5B. Right panels: disk with the same sectors rearranged, 5G, 5RP, 5YR, 5B. The disk represented in the left panels produced strikingly different colors when spun in opposite directions, while the disk represented in the right panels produced very little difference. The plotted sine-waves are the Fourier fundamentals of the cone stimulation produced by each disk: ΔL/L − ΔM/M (top panels) and ΔS/S (bottom panels). The two stimulus fundamentals in the left panel, for the first disk, are 129° out of phase, while the two fundamentals in the right panel, for the second disk, are 174° out of phase (almost in antiphase).

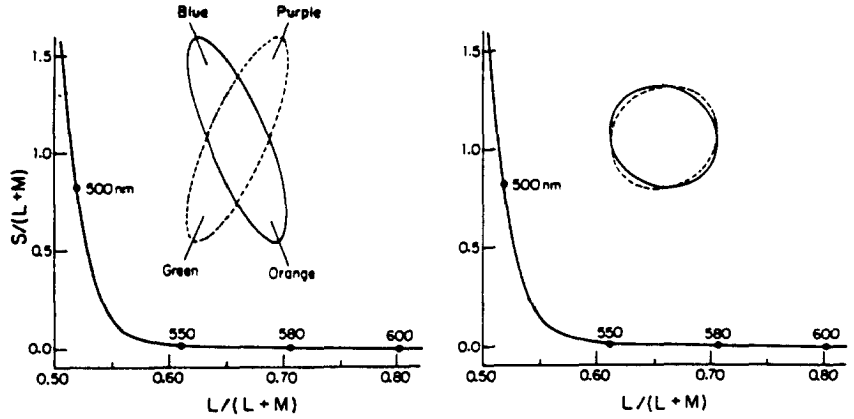


Fig. 9. The MacLeod–Boynton diagram depicts the effective chromaticity of the two color disks (Fig. 8), each spinning in two opposite directions. Left panel: disk 5RP, 5YR, 5G, 5B; right panel: disk 5G, 5RP, 5YR, 5B. Each ellipse represents the vector sum of the two Fourier fundamentals of the cone stimulation shown in Fig. 8, assuming that the disk is spinning sufficiently fast for the S signal to lag L − M by 90° (relative to the phase lag of the stimulus fundamentals). The two ellipses in the left panel have different tilts that correspond to the different colors seen on the disk 5RP, 5YR, 5G, 5B when spun in opposite directions. The two ellipses in the right panel are nearly identical, explaining why disk 5G, 5RP, 5YR, 5B appears similar when spun in opposite directions.

antiphase for the opposite direction of rotation. The total phase difference between the S and L − M signals is the sum of the stimulus phase difference $\phi$ and the physiological phase difference $\theta$. Reversing the direction of rotation changes the sign of $\phi$ but leaves $\theta$ unaffected, so that the total phase difference is $\theta + \phi$ for one direction of rotation and $\theta - \phi$ for the other. If we assume that the physiological phase lag of the S signal is $\theta = 90°$, then the resultant stimulation for the two directions of rotation are represented by the two ellipsoidal trajectories in the left panel of Fig. 9. The ellipses are Lissajous figures depicting the vector sum of the two stimulus fundamentals given the 129° phase difference of the stimuli ($\phi$), and assuming the additional 90° lag of the S signal ($\theta$). The effective chromaticity moves around the path of each ellipse at the rate the disk spins, but in opposite directions for the two ellipses, corresponding to the two directions of spin. The major axis of one ellipse is in the orange and blue direction (for the B, G, YR, RP sequence) and the axis of the other ellipse is in the green and purple direction (for the opposite spin sequence, RP, YR, G, B). The end-points of the two major axes correspond to the chromaticity of Munsell chips (value 6) of 7YR and 4B, and of 1G and 1RP, respectively. The matching chips that Spillmann's observers selected (Table 3) for the rotating disk were not too dissimilar: 2.5YR and 2.5B; 10G and 7.5RP. Thus the present analysis largely accounts for the difference in appearance when the disk is rotated in opposite directions.

Spillmann (1990) observed that after simply rearranging the four Munsell sectors in a different sequence, 5G, 5RP, 5YR, 5B, the disk appeared similar for the two directions of rotation. This result can be readily understood by the same analysis. For this sequence, the stimulus Fourier fundamentals, $\Delta L/L - \Delta M/M$ and $\Delta S/S$ are 174° out of phase (almost in antiphase—Fig. 8, right panels), and the amplitude of the S Fourier fundamental is also reduced compared to the left panel. (The large second harmonic should have little effect since it occurs above ~15 Hz.) If we again assume that the disk is spun sufficiently fast for the S signal to lag the L signal by an additional 90°, then the S and L − M signals would nearly be in quadrature phase with respect to each other. The sum of the S and L − M Fourier fundamentals representing the two directions of disk spin (and assuming the physiological 90° S lag) are shown by the ellipses in the right panel of Fig. 9. The two ellipses are almost identical, and thus spinning the disk in opposite directions produces highly similar colors. (If the two fundamentals were precisely in-phase or in antiphase initially, then any phase lag $\theta$ of the S signal would result in coincident ellipses for the two directions of spin, because $\theta + 0°$ and $\theta - 0°$, or $\theta + 180°$ and $\theta - 180°$, specify identical pairs of ellipses regardless of the value of $\theta$. The second disk approximates the antiphase condition.)

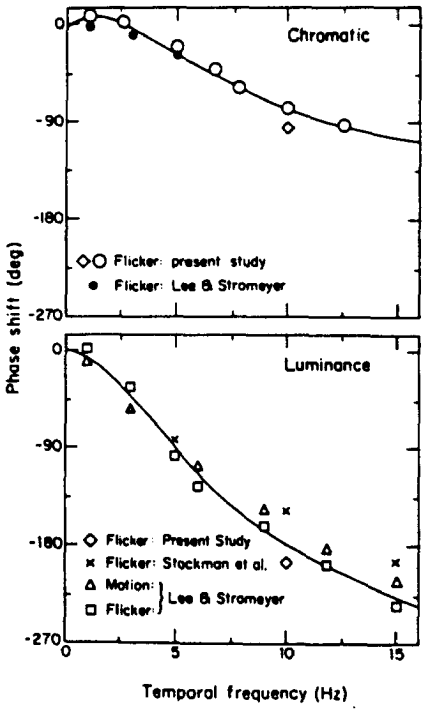


Fig. 10. Summary of S cone phase measurements from various studies. The top panel represents the relative phase shift of the S signal as measured with the chromatic discrimination paradigm: open circles—mean data from the present study; solid circles—Stromeyer and Lee (1989). The bottom panel represents the relative phase shift of the S signal for luminance flicker or motion discrimination: squares and triangles—Lee and Stromeyer (1989); crosses—Stockman et al. (1987). The diamonds are data from our Fig. 6, interpolated for and S cone light-adaptation level of 8.54 log quanta·deg$^{-2}$·sec$^{-1}$ (re 441 nm)—the same adapting level as for the solid circles, squares and triangles (re 441 nm) and for the crosses (re 435 nm). For the open circles the level was 8.80 log quanta·deg$^{-2}$·sec$^{-1}$ (re 441 nm). The smooth curves are described in the text.

In this discussion, we have assumed a 90° phase lag of the S signal, in addition to the stimulus phase shifts. When $\theta = 90°$, the two spin directions produce mirror symmetric ellipses. The actual physiological phase lag in Spillmann's (1990) experiment would of course vary with temporal frequency (spin rate) and adaptation conditions. Since he chose a temporal frequency that maximized the difference in color appearance for the two directions of rotation, we may assume that the S lag is approximately 90°, but the precise value is not important for our analysis.

This simple analysis also helps to understand the general shape of our phase discrimination template (Fig. 4). For simplicity assume there is no physiological phase shift between the S and L − M signals ($\theta = 0°$). Then the maximal sensitivity, at the template minima, represents a discrimination between two intervals where the S and L − M signals are, respectively, in-phase and in antiphase, in which case the two ellipses degenerate into two straight lines with different tilts. In the chromaticity diagram, this represents a discrimination between a straight, slightly reddish and greenish vector and a straight, slightly bluish and orangish vector. At the peak of the template, where sensitivity is minimal, the S and L − M signals are in quadrature phase. The task is represented by a discrimination between the two directions around an ellipse inscribing the S and L − M vectors—the same ellipse for the two intervals.

*Phase measurements: evidence for multiple S cone pathways*

The present phase measurements of the S signal relative to L and M, obtained with a chromatic discrimination criterion, are very different from measurements obtained with a luminance flicker or motion criterion (Stockman et al., 1987; Lee & Stromeyer, 1989). The disparate results provide evidence that S cone signals feed into separate chromatic and luminance pathways. Figure 10 summarizes results from several studies. Violet and red tests on an intense yellow-green or orange adapting field stimulated the S and L cones, respectively. Figure 10 shows the lag (or lead—positive phase shifts) of the S signal relative to the L signal as a function of temporal frequency. Each datum point (except crosses) is based on a complete phase template, and represents mean results for two or three observers.

The upper panel shows data with the chromatic discrimination criterion: open circles plot results of the present experiment (Fig. 5), in which violet light was flickered relative to equiluminant red–green light; solid circles plot earlier measurements where violet was flickered relative to red (Lee & Stromeyer, 1989). The adapting level for the S cones was equivalent to 8.80 (open circles) and 8.54 (solid circles) log quanta·deg$^{-2}$·sec$^{-1}$ at 441 nm. The solid curve is the same phase transfer function plotted in Fig. 5.

The *same* violet and red flickering stimuli used for the chromatic discrimination paradigm (solid circles) were also used to measure templates with the luminance discrimination paradigm (squares in lower panel, from Lee & Stromeyer, 1989). The triangles were obtained with a direction identification paradigm, in which the uniform violet and red flicker was

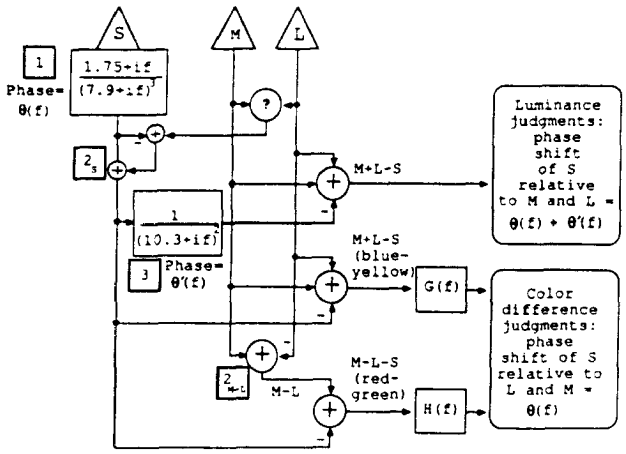


Fig. 11. An opponent-color model for the phase discrimination data. Signals from the three cone types (S, M, L) feed into three opponent mechanisms: red–green chromatic, blue–yellow chromatic and luminance. There are two sites for gain and phase changes in the S cone pathways. Site 1 causes phase lag $\theta$ and may occur at the S cones *per se*. The phase lag at site 3, $\theta'$, adds with the first phase lag, $\theta$, to produce a greater lag for the S input to luminance than for the S input to chromatic judgments. See text for other features.

replaced with vertical, violet and red, counter-phase flickering gratings in spatial quadrature phase (Lee and Stromeyer, 1989). The diamonds represent the present flicker results from Fig. 6, interpolated for a level of 8.54 log quanta·deg$^{-2}$·sec$^{-1}$ at 441 nm. Finally, the crosses represent results of Stockman et al. (1987 and personal communication) for violet and red flickering lights whose phase was adjusted to achieve a photometric flicker null. Results have again been interpolated for an S cone adapting level of 8.54 log quanta·deg$^{-2}$·sec$^{-1}$ at 435 nm—similar to the level at which the squares and triangles were obtained. For luminance and motion detection, the S signal is inverted with respect to L and M (Stockman et al., 1987; Lee & Stromeyer, 1989). This additional 180° "phase shift" of S cones opposing M cones is not represented in either panel of Fig. 10, since the figure only shows the component of the S cone lag which varies with temporal frequency. Our model, presented later, makes explicit the role of opponency in these phase relationships.

The phase data in the lower panel are fitted with a transfer function of real zeros and negative real poles. There is a single zero at $f = 1.75$ Hz and a quintuple pole at 7.9 Hz for a transfer function of $(1.75 + if)/(7.9 + if)^5$. There is agreement between the zero and pole locations for the luminance and chromatic mechanisms (top panel). (However, the two transfer functions were obtained at slightly different S cone adapting levels, i.e. 0.26 log units difference; the values would change slightly for matched adapting levels—see next section.) While the zero is required for the chromatic phases in order to reproduce the phase advance at low frequencies, the luminance phases contain no actual phase advance but only a negative second derivative at low frequencies, indicating the need for the zero. Because there are four more poles than zeros, the asymptotic high-frequency phase lag is 360° for the luminance mechanism.

Because the S cone contribution to luminance has a negative sign at zero frequency, it might be argued that the nominal luminance discrimination was actually a yellow–blue judgment. However, we showed that when observers are asked to make luminance or yellow–blue judgments with identical stimuli, two widely separated templates are obtained (Fig. 7). The phase measurements thus indicate that S cone signals contribute to separate mechanisms that mediate luminance and chromatic information. Stockman et al. (1987), using a selective temporal masking paradigm, also separated two S cone mechanisms that process luminance and chromatic information.

### *Model of the opponent pathways*

We shall first consider a model for the different S cone phase lags, and then consider

"second-site" adaptational effects, which further specify the processing-stages of the model.

*The phase lags.* Figure 11 is an elaboration of a standard opponent-color model (Boynton, 1979), containing two chromatic mechanisms (red–green and blue–yellow) and one luminance mechanism. The cone signals affect the blue–yellow and luminance mechanisms in a similar manner: S signals oppose summed, M + L signals. In the red–green mechanism, S signals oppose M and support L. Thus for each mechanism, the S signal is shown inverted relative to M.

Because our measurements are of S *relative* to L and M, we need consider only gain and phase changes in S cone pathways. The first phase shift, $\theta$, is assumed to occur at site 1, which may include the S cones themselves. The phase of the transfer function at site 1 is shown in Figs 5 and 10 (top). The transfer function specified at site 1 is for an S cone adaptation level of 8.80 log quanta·deg$^{-2}$·sec$^{-1}$ (re 441 nm); light adaptation would presumably change the pole and zero values at site 1, and thus change the relative S cone phase for all mechanisms. There are two reasons for postulating a phase change at site 1, before the S signal has combined with M and L. First, the chromatic templates measured at 3 Hz peaked at 260–272° whether the red and green lights were in antiphase and stimulated the red–green mechanism (Fig. 3), or were in-phase and stimulated the blue–yellow mechanism (Fig. 7). Second, varying the S cone light-adaptation level had similar effects on the luminance and chromatic templates (Fig. 6). The change of lag caused by light adaptation may occur within the S cones, for the electrical response of cones becomes faster with increased light adaptation (Baylor & Hodgkin, 1974; Baron & Boynton, 1975), and all three cone types appear to have similar temporal properties (Baylor, 1986; Crognale & Jacobs, 1988).

The model also postulates a second phase change $\theta'$, at site 3, near where the S signal is combined with the summed M + L signal within the luminance mechanism. Therefore the total S cone phase shift is $\theta$ for the chromatic task, and $\theta + \theta'$ for the luminance (or motion) task. The data of Fig. 6 indicate that $\theta' \cong 100°$ at 10 Hz. [This second S lag, $\theta'$, could alternatively be replaced with an equivalent *advance* of the L and M cone signals feeding into the luminance mechanism, produced by a temporal differentiating circuit (see MacLeod, 1978).] The transfer function for site 3 is for the same S cone adapting level considered for site 1 (8.80 log quanta·deg$^{-2}$·sec$^{-1}$). For this adapting level, the transfer function in the bottom of Fig. 10 would change to approximately $(1.75 + if)/(7.9 + if)^3(10.3 + if)^2$, estimated from Fig. 6. The factors in the denominator correspond sequentially to the 3 poles at site 1 and the 2 poles at site 3.

The luminance mechanism is apparently faster than either chromatic mechanism, as shown by both measurements of temporal MTFs (Kelly & van Norren, 1977; Wisowaty, 1981) and reaction times (Schwartz & Loop, 1982). To avoid the misleading impression that the *absolute* phases of the luminance and chromatic mechanism differ by $\theta'$, we have postulated additional filters G(f) and H(f). Their purpose is to make the chromatic mechanisms slower than the luminance one, despite the fact that the S cone input to the chromatic mechanism is less delayed than the S cone input to luminance. Recordings of macaque retinal ganglion cells (Lee, Martin & Valberg, 1989) and LGN cells (DePriest, Sclar & Lennie, 1988) with chromatic flicker suggest that this additional filtering occurs central to these cells.

*"Second-sites" for chromatic adaptation.* The model also postulates "second-sites" to account for chromatic adaptation within both the S pathways (Fig. 11, site $2_S$) and the M − L pathway (site $2_{M-L}$). These early adaptational sites must precede higher level opponent sites in the model, for reasons given below.

In transient tritanopia the threshold for a test flash detected by the S cones is elevated by dimming an intense yellow adapting field, which itself produces few quantal catches in the S cones (Pugh & Mollon, 1979). Transient tritanopia also occurs in identifying the direction of motion of an S cone grating mediated via the luminance mechanism (Lee & Stromeyer, 1989). Thus transient tritanopia affects both the chromatic mechanisms and the luminance mechanism. Because transient tritanopia is often a large effect, we presume that both red–green and yellow–blue mechanisms are affected.

The second-site $2_S$ produces a gain reduction of the S signal depending on the difference of S signals and some combination of M and L signals. The gain reduction is spectrally opponent, as shown by measurements of transient tritanopia with mixed short and long wave adapting fields (Augenstein & Pugh, 1977), and by measurements of "combinative euchroma-

topsia", in which S cone test sensitivity on short wave adapting fields is restored by adding a long wave adapting field (Polden & Mollon, 1980). Both M and L signals oppose S at the opponent site (Mollon & Polden, 1979; Polden & Mollon, 1980). In Fig. 11 we show that the gating at site $2_S$ is opponent, but that the output contains just the S signal and is therefore non-opponent.

Second-site adaptation also occurs in the M − L pathway, as shown by measurements of transient protanopia (Reeves, 1981) and combinative euchromatopsia (Stromeyer et al., 1985), and these processes are postulated to occur at site $2_{M-L}$.

Short-wave redness produced by adapting the S cones with steady (Stromeyer & Lee, 1988) and temporally modulated fields (Krauskopf et al., 1982; Mollon & Cavonius, 1987) has little effect on chromatic discrimination mediated by the M − L signals. This led Mollon and Cavonius (1987) to conclude that the M − L pathway measured at threshold does not correspond to the Hering-type opponent mechanism responsible for color appearance (Hurvich & Jameson, 1957). However, direct "test" interactions of S and M − L signals have been clearly demonstrated by Boynton et al. (1983), and Boynton, Nagy and Eskew (1986), which is consistent with the S cone contribution to the red–green mechanism found in the present study. The model in Fig. 11 attempts to reconcile these disparate results by postulating an early second-site, site $2_{M-L}$ controlled by M − L modulation (with no S input). Adaptation effects may occur largely at this early site, while test stimuli, representing all three cone classes, may produce interactions at a higher opponent site.

## CONCLUSIONS

The model explains the different colors seen with the spinning color disk, without recourse to the inhibitory interactions postulated by Spillmann and Neumeyer (1984). The model is consistent with what is known about the effects of S cone adaptation level on the contribution of the S cones to chromatic, luminance flicker, and motion judgments. The model is also consistent with the view that the opponent mechanisms isolated at threshold are transformed by successive stages into the Hering-type opponent mechanisms responsible for the appearance of colors.

*Acknowledgements*—Research supported by Grants NIH EY-01808, AFOSR 86-0338 and DFG SFB325-B4. We thank Drs B. Drum, R. Humanski, J. Mollon, A. Reeves and A. Stockman for their helpful comments.

## REFERENCES

Augenstein, E. J. & Pugh, E. N. Jr (1977). The dynamics of the $\Pi_1$ colour mechanism: Further evidence for two sites of adaptation. *Journal of Physiology, London, 272*, 247–281.

Baron, W. S. & Boynton, R. M. (1975). Response of primate cones to sinusoidally flickering homochromatic stimuli. *Journal of Physiology, London, 246*, 311–331.

Baylor, D. A. (1986). Photoreceptor signals and vision. *Investigative Ophthalmology and Visual Science (Suppl.), 28*, 34–49.

Baylor, D. A. & Hodgkin, A. L. (1974). Changes in time scale and sensitivity in turtle photoreceptors. *Journal of Physiology, London, 242*, 729–758.

Boynton, R. M. (1979). *Human color vision*. New York: Holt, Rhinehart & Winston.

Boynton, R. M. & Kambe, N. (1980). Chromatic difference steps of moderate size measured along theoretically critical axes. *Color Research and Application, 5*, 13–23.

Boynton, R. M., Nagy A. L. & Olson, C. X. (1983). A flaw in equations for predicting chromatic differences. *Color Research and Application, 8*, 69–74.

Boynton, R. M., Nagy, A. L. & Eskew, R. T. Jr (1986). Similarity of normalized discrimination ellipses in the constant-luminance chromaticity plane. *Perception, 15*, 755–763.

Crognale, M. & Jacobs, G. H. (1988). Temporal properties of the short-wavelength cone mechanism: Comparison of receptor and postreceptor signals in the ground squirrel. *Vision Research, 28*, 1077–1082.

Davidoff, J. B., Aspinall, P. A. & Hill, A. R. (1978). A new colour flicker phenomenon. *Modern Problems in Ophthalmology, 19*, 187–189.

DePriest, D. D., Sclar, G. & Lennie, P. (1988). Central limits to chromatic flicker-sensitivity. *Investigative Ophthalmology and Visual Science (Suppl.), 29*, 326.

Drum, B. (1989). Hue signals from short- and middle-wavelength-sensitive cones. *Journal of the Optical Society of America, A6*, 153–157.

Eisner, A. & MacLeod, D. I. A. (1981). Flicker photometric study of chromatic adaptation: Selective suppression of cone inputs by colored backgrounds. *Journal of the Optical Society of America, 71*, 705–718.

Hartridge, H. (1949). *Colours and how we see them*. London: Bell.

Hill, A. R., Rodger, G. & Smalridge, L. (1980). Some further observations on the colour flicker phenomenon. In Verriest, G. (Ed.), *Colour vision deficiencies V*. Bristol: Adam Hilger.

Hurvich, L. M. & Jameson, D. (1957). An opponent-process theory of color vision. *Psychological Review, 64*, 384–404.

Kelly, D. H. & van Norren, D. (1977). Two-band model of heterochromatic flicker. *Journal of the Optical Society of America, 67*, 1081–1091.

Krauskopf, J., Williams, D. R. & Heeley, D. W. (1982). Cardinal directions of color space. *Vision Research, 22*, 1123–1131.

Lee, B. B., Martin, P. R. & Valberg, A. (1989). Sensitivity of macaque retinal ganglion cells to chromatic and luminance flicker. *Journal of Physiology, London, 414*, 223–243.

Lee, J. & Stromeyer, C. F. III (1989). Contribution of human short-wave cones to luminance and motion detection. *Journal of Physiology, London, 413,* 563–593.

Lindsey, D. T., Pokorny, J. & Smith, V. C. (1986). Phase-dependent sensitivity to heterochromatic flicker. *Journal of the Optical Society of America, A3,* 921–927.

MacLeod, D. I. A. (1978). Visual sensitivity. *Annual Review of Psychology, 29,* 613–645.

MacLeod, D. I. A. & Boynton, R. M. (1979). A chromaticity diagram showing cone excitation by stimuli of equal luminance. *Journal of the Optical Society of America, 69,* 1183–1186.

Middleton, W. E. K. & Holmes, M. C. (1949). The apparent colors of surfaces of small subtense—a preliminary report. *Journal of the Optical Society of America, 39,* 582–592.

Mollon, J. D. (1982). A taxonomy of tritanopias. In Verriest, G. (Ed.), *Documenta ophthalmologica, proceeding series* (Vol. 33). The Hague: Junk.

Mollon, J. D. & Cavonius, C. R. (1987). The chromatic antagonisms of opponent process theory are not the same as those revealed in studies of detection and discrimination. In Verriest, G. (Ed.), *Colour vision deficiencies VIII.* Dordrecht: Junk.

Mollon, J. D. & Polden, P. G. (1979). Post-receptoral adaptation. *Vision Research, 19,* 435–440.

Newhall, S. M., Nickerson, D. & Judd, D. B. (1943). Final report of the O.S.A. subcommittee on spacing of the Munsell colors. *Journal of the Optical Society of America, 33,* 385–418.

Pokorny, J., Smith, V. C. & Lund, D. (1978). Technical characteristics of 'Color-test glasses'. *Modern Problems in Ophthalmology, 19,* 110–112.

Polden, P. G. & Mollon, J. D. (1980). Reversed effect of adapting stimuli on visual sensitivity. *Proceedings of the Royal Society of London, B 210,* 235–272.

Pugh, E. N. Jr & Mollon, J. D. (1979). A theory of the $\pi_1$ and $\pi_3$ color mechanisms of Stiles. *Vision Research, 19,* 293–312.

Reeves, A. (1981). Transient desensitization of a red-green opponent site. *Vision Research, 21,* 1267–1277.

Schwartz, S. H. & Loop, M. S. (1982). Evidence for transient luminance and quasi-sustained color mechanisms. *Vision Research, 22,* 445–447.

Smith, V. C. & Pokorny, J. (1975). Spectral sensitivity of the foveal cone photopigments between 400 and 500 nm. *Vision Research, 15,* 161–171.

Spillmann, L. (1974). Different color sensations caused by temporal interaction between hues of equal brightness and saturation. *Pflügers Archiv, European Journal of Physiology, 347,* R58, Abstr. 116.

Spillmann, L. (1990). Wahrgenommene Bunttonunterschiede auf gegenläufigen Farbkreiseln. *Farbe und Design, 49/50,* 18–24.

Spillmann, L. & Neumeyer, C. (1984). Änderung der Farbwahrnehmung bei gegensinniger Abfolge der Farbtöne im Farbenkreis. In Spillmann, L. & Wooten, B. R. (Eds.), *Sensory experience, adaptation, and perception: Festschrift for Ivo Kohler.* Hillsdale, N.J.: Lawrence Erlbaum.

Stiles, W. S. (1953). Further studies of visual mechanisms by the two-colour threshold method. In *Coloquio sobre problemas opticos de la vision* (Vol. 1, pp. 65–103). Madrid: Union Internationale de Physique Pure et Appliquée.

Stockman, A., MacLeod, D. I. A. & DePriest, D. D. (1987). An inverted S-cone input to the luminance channel: Evidence for two processes in S-cone flicker detection. *Investigative Ophthalmology and Visual Science (Suppl.) 28,* 92.

Stromeyer, C. F. III & Lee, J. (1988). Adaptational effects of short wave cone signals on red-green chromatic detection. *Vision Research, 28,* 931–940.

Stromeyer, C. F. III, Cole, G. R. & Kronauer, R. E. (1985). Second-site adaptation in the red-green chromatic pathways. *Vision Research, 25,* 219–237.

Stromeyer, C. F. III, Cole, G. R. & Kronauer, R. E. (1987). Chromatic suppression of cone inputs to the luminance flicker mechanism. *Vision Research, 27,* 1113–1137.

Thornton, J. E. & Pugh, E. N. Jr (1983a). Relationship of opponent-colours cancellation measures to cone-antagonistic signals deduced from increment threshold data. In Mollon, J. D. & Sharpe, L. T. (Eds.), *Color vision, physiology and psychophysics.* New York: Academic.

Thornton, J. E. & Pugh, E. N. Jr (1983b). Red/green opponency at detection threshold. *Science, New York, 219,* 191–193.

Wetherill, G. B. (1963). Sequential estimation of quantal response curves. *Journal of the Royal Statistical Society, B25,* 1–48.

Wisowaty, J. J. (1981). Estimates for the temporal response characteristics of chromatic pathways. *Journal of the Optical Society of America, 71,* 970–977.

Wyszecki, G. & Stiles, W. S. (1982). *Color science: concepts and methods, quantitative data and formulas* (2nd edn). New York: Wiley.